Jurnal Teknologi

Full Paper

STRUCTURE AND DIELECTRIC PROPERTIES OF POLYPROPYLENE CONTAINING ZINC IRON OXIDE NANOFILLER

Salma Nurdina[a], Aizat Azmi*, Norhafezaidi Mat Saman, Lau Kwan Yiew

Faculty of Electrical Engineering, Engineering Campus, Universiti Teknologi Malaysia, 81310 UTM Johor Bahru, Johor, Malaysia

Article history
Received
14 February 2025
Received in revised form
25 April 2025
Accepted
29 May 2025
Published Online
27 February 2026

*Corresponding author
aizat.azmi@utm.my

Graphical abstract

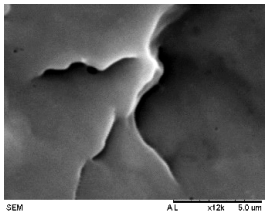

(a)

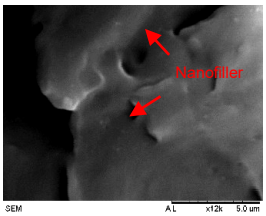

(b)

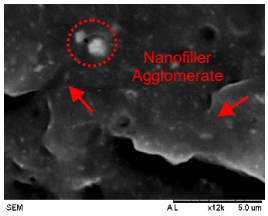

(c)

Figure 1 Morphology Images of (a) pure PP with uniform dispersion, (b)PP with 0.5 wt.% nanofillers showing uniform dispersion, and (c)PP with 5 wt.% nanofillers exhibiting agglomeration.

Abstract

Cross-linked polyethylene (XLPE) is commonly used in high-voltage cable insulation due to its favorable dielectric properties. However, its thermoset nature limits recyclability and thermal performance. Polypropylene (PP), a recyclable thermoplastic, offers better thermal stability, making it a potential alternative. Despite this, PP's dielectric performance under high-voltage conditions can be insufficient, especially when filled with single metal oxide nanofillers that absorb moisture. Zinc iron oxide ($ZnFe_2O_4$), a multi-metal oxide with low moisture absorption and thermal stability, may offer a solution, yet its application in PP nanocomposites remains underexplored. This study investigates the structural, thermal, and dielectric characteristics of PP/$ZnFe_2O_4$ nanocomposites with 0.5, 1, 2, and 5 wt.% filler content. SEM and DSC analyses revealed improved crystallization behavior with $ZnFe_2O_4$ acting as a nucleating agent. Good nanoparticle dispersion was observed at lower filler loadings, while higher content led to agglomeration. AC and DC breakdown strength tests (ASTM D149, D3755) showed pure PP had the highest strength (158 ± 8 kV/mm AC; 327 ± 10 kV/mm DC). The 0.5 wt.% sample exhibited comparable values, while 5 wt.% resulted in the lowest performance (144 ± 10 kV/mm AC; 203 ± 23 kV/mm DC). These findings confirm that low $ZnFe_2O_4$ content enhances PP's thermal and dielectric properties for potential HV insulation applications.

Keywords: Polypropylene nanocomposites, Zinc iron oxide, Dielectric performance, Breakdown strength, Nanofiller effects

Abstrak

Polietilena silang (XLPE) banyak digunakan sebagai penebat kabel voltan tinggi kerana sifat dielektriknya yang baik. Namun, sifat termoset XLPE menghadkan kebolehkitar semula dan kestabilan terma pada suhu tinggi. Polipropilena (PP), sejenis termoplastik yang boleh dikitar semula, menawarkan kestabilan terma yang lebih baik dan berpotensi menggantikan XLPE. Walau bagaimanapun, prestasi dielektrik PP kurang memuaskan di bawah tekanan elektrik tinggi, terutamanya apabila diisi dengan pengisi nano oksida logam tunggal yang menyerap lembapan. Zink ferit ($ZnFe_2O_4$), oksida berbilang logam dengan penyerapan lembapan rendah dan kestabilan tinggi, berpotensi mengatasi masalah ini, namun masih kurang dikaji dalam nanokomposit berasaskan PP. Kajian ini menilai struktur, sifat terma, dan prestasi dielektrik PP/$ZnFe_2O_4$ dengan kandungan 0.5, 1, 2, dan 5 wt.%. Analisis SEM dan DSC menunjukkan $ZnFe_2O_4$ bertindak sebagai agen penghabluran dan meningkatkan suhu penghabluran. Dispersi baik diperoleh pada kandungan rendah, manakala aglomerasi berlaku pada kandungan tinggi. Kekuatan tembus AC dan DC tertinggi diperoleh pada PP tulen (158 ± 8 kV/mm AC; 327 ± 10 kV/mm DC), manakala 0.5 wt.% menunjukkan prestasi hampir setara. Kandungan 5 wt.% menghasilkan kekuatan terendah akibat aglomerasi. Kesimpulannya, penambahan $ZnFe_2O_4$ dalam jumlah kecil meningkatkan sifat terma dan mengekalkan prestasi dielektrik yang baik.

Kata kunci: Nanokomposit polipropilena, Zink ferum oksida, Prestasi dielektrik, Kekuatan penembusan, Kesan pengisi nano

1.0 INTRODUCTION

The rapid growth of power generation and transmission technologies has driven the need for advanced insulation materials to ensure efficient and reliable operation under HV conditions. To date, cross-linked polyethylene (XLPE) is widely used as an insulation material in HV alternating current (HVAC) and HV direct current (HVDC) cables due to its low permittivity, high dielectric strength, low dielectric loss, and good thermo-mechanical properties at operating temperatures up to around 90°C [1]. However, XLPE has notable limitations, including the formation of by-products during the crosslinking process, limited thermal performance above 90°C, and poor recyclability due to its thermoset nature. These drawbacks can affect long-term dielectric performance. Moreover, the manufacturing process requires additional degassing steps, making production more time-consuming [2].

In contrast, polypropylene (PP) has emerged as a promising alternative insulation material. Its excellent mechanical properties, high thermal stability, chemical resistance, and ease of processing are attributed to its thermoplastic nature [3, 4, 5]. Notably, PP exhibits a higher melting temperature, typically exceeding 150°C, compared to XLPE, which becomes unstable above 105°C [6]. These attributes make PP a promising candidate for insulation applications in modern HV systems. However, despite its many advantages, the dielectric performance of PP remains a concern in HV applications, especially under prolonged thermal and electrical stress. To overcome these limitations, researchers have explored the incorporation of nanofillers to enhance the thermal, mechanical, and dielectric properties of PP [7]. While several studies have shown promising improvements, investigations on the dielectric behavior of PP-based nanocomposites under different electric field conditions are still relatively limited.

Encouraging findings have been reported in the literature. For example, *Sharip et al.* [8] demonstrated that incorporating 1 wt.% magnesium oxide (MgO) nanofiller into a polypropylene/ethylene-octene copolymer (PP/EOC10) blend significantly improved its AC breakdown strength, reaching up to 175 kV/mm, which is higher than that of pure PP. Similarly, *Banerjee et al*. [9] reported that adding 1–5 wt.% zinc oxide (ZnO) nanofillers enhanced both the dielectric permittivity and AC breakdown strength of PP nanocomposites, primarily due to interfacial polarization effects. In another study, *Zhao et al.* [10] observed a 32% increase in DC breakdown strength with the addition of 3 wt.% MgO nanofillers to PP. These results highlight the potential of nanofillers to effectively improve the dielectric properties of polypropylene for HV insulation applications.

Unfortunately, some studies have found shortcomings in single-metal oxide nanofillers, such as agglomeration and increased water adsorption as a result of the surface hydroxyl groups [11, 12]. Similar issues with single-metal oxide nanofillers, particularly TiO_2, which also has surface hydroxyl groups that encourage agglomeration, have been reported by *Chong et al.* [13]. These issues are known to increase the permittivity and loss of tangent while diminishing the breakdown strength [14, 15, 16]. In contrast, the multi-element oxide nanofillers are more advantageous. *Azmi et al.* [17, 18, 19] showed that nanofillers such as magnesium aluminate ($MgAl_2O_4$) and calcium carbonate ($CaCO_3$) improve the thermal, mechanical, and dielectric stability and reduce agglomeration and moisture-induced degradation after thermal aging at high temperatures.

Zinc iron oxide ($ZnFe_2O_4$) as one of the multi-element oxides is cubical spinel structured and has a particle size of less than 100 nm. It finds application in supercapacitors, batteries, and catalytic systems [20]. Its ability to enhance the thermal and dielectric properties of polymer nanocomposites was demonstrated by *Raju et al.* [21], who also reported an improvement in thermal stability with an increase in $ZnFe_2O_4$ concentration. However, it remains to be investigated how effective $ZnFe_2O_4$ is in dielectric aspects of PP-based nanocomposites in HV conditions.

This study investigates the structure, thermal behavior, and dielectric performance of PP/$ZnFe_2O_4$ nanocomposites with varying zinc iron oxide content (0.5, 1, 2, and 5 wt.%). Morphological characteristics and thermal behavior were analyzed using scanning electron microscopy (SEM) and differential scanning calorimetry (DSC), while AC and DC breakdown strengths were measured in accordance with ASTM standards. The findings contribute valuable insights toward the development of next-generation HV insulation materials with improved thermal and dielectric performance.

2.0 METHODOLOGY

This section makes it clear how PP/$ZnFe_2O_4$ nanocomposites (with varying weight concentrations of 0.5, 1, 2, and 5 wt.%) were synthesized. It also explains how scanning electron microscopy (SEM) and differential scanning calorimetry (DSC) were utilized to characterize the morphology and the thermal properties of the materials. Moreover, both AC and DC breakdown strength tests were performed for the materials in order to assess their dielectric properties.

A. Experimentation

The polypropylene (PP) used in this study consisted of a 50:50 ratio of isotactic polypropylene homopolymer (PPh), TitanPro 6531M, and polypropylene impact copolymer (PPi), TitanPro SM340, which both materials were both sourced from Lotte Chemical

Titan. Zinc iron oxide ($ZnFe_2O_4$) nanopowder, with a particle size of less than 100 nm, was obtained from Sigma Aldrich and used as the nanofiller. Nanocomposites were prepared by incorporating $ZnFe_2O_4$ into the PP matrix at filler loadings of 0.5, 1, 2, and 5 wt.%. The mixing process was carried out using a Brabender Melt Mixer, with each formulation consisting of 35 grams of material. The specific compositions are detailed in Table 1.

Table 1 Composition of Polypropylene Blends and PP/$ZnFe_2O_4$ Nanocomposites for Sample Preparation

Materials	Weight (g)				
	0wt.%	0.5wt.%	1wt.%	2wt.%	5wt.%
Polypropylene Homopolymer	17.5	17.41	17.325	17.15	16.625
Polypropylene Impact Copolymer	17.5	17.41	17.325	17.15	16.625
Zinc Iron Oxide	-	0.175	0.35	0.70	1.75
Total	35	35	35	35	35

All materials were dried at 70°C for 24 hours to remove moisture before blending. The sample preparation steps are illustrated in Figure 2.

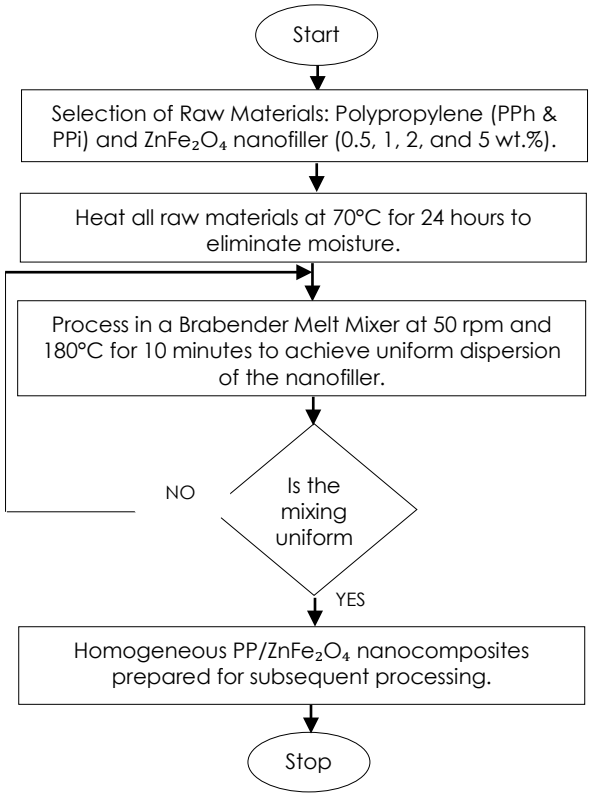

Figure 2 Flowchart of Sample Preparation

The notations on the samples that have been prepared were assigned in an overly simplistic manner; they were labeled "P/C" for the polymer type and nanofiller content, respectively. Table 2 shows the various sample formulations along with their respective labels.

Table 2 Sample Labeling System and Compositions for Polypropylene Blends and Nanocomposites

Samples (P/C)	Polymer (P)	Nanofiller content (C)
PP/0	PPh + PPi	-
PP/$ZnFe_2O_4$/0.5	PPh + PPi	0.5 wt.% $ZnFe_2O_4$
PP/$ZnFe_2O_4$/1	PPh + PPi	1 wt.% $ZnFe_2O_4$
PP/$ZnFe_2O_4$/2	PPh + PPi	2 wt.% $ZnFe_2O_4$
PP/$ZnFe_2O_4$/5	PPh + PPi	5 wt.% $ZnFe_2O_4$

The samples were pressed into thin films through the use of a Carver Hydraulic Press, resulting in a thickness of 100 ± 5 µm. The temperature was set to 180 °C and maintained at that temperature for 2 minutes to preheat the specimens, after which a 2-ton load was applied for another 2 minutes. The diameter of each thin film specimen was around 9 cm. The specimens were then cooled to room temperature under ambient conditions before further characterization.

B. Differential Scanning Calorimetry

The thermal properties of the nanocomposites were analyzed using a Perkin Elmer DSC6 differential scanning calorimeter (DSC) under controlled conditions, with testing performed according to the differential scanning calorimetry method from Mettler Toledo. As shown in Figure 3, the setup and procedure for the DSC analysis are depicted.

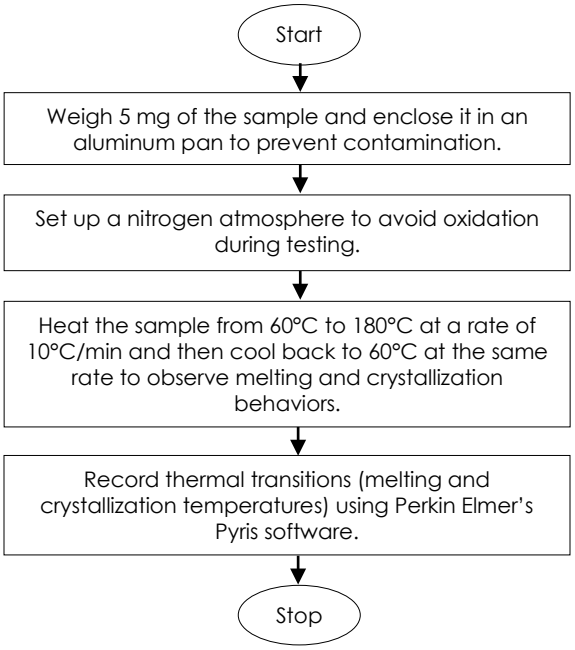

Figure 3 Flowchart of DSC Analysis Testing

DSC was selected to determine the melting point and the crystallinity of the nanocomposites, which are essential parameters influencing their thermal and dielectric performance.

C. Scanning Electron Microscopy

To examine the morphology, structure, and dispersion of nanofillers in the polypropylene matrix, the researchers utilized a scanning electron microscope (SEM) Model Hitachi TM3000. The procedure for SEM imaging follows a stepwise approach, as illustrated in Figure 4.

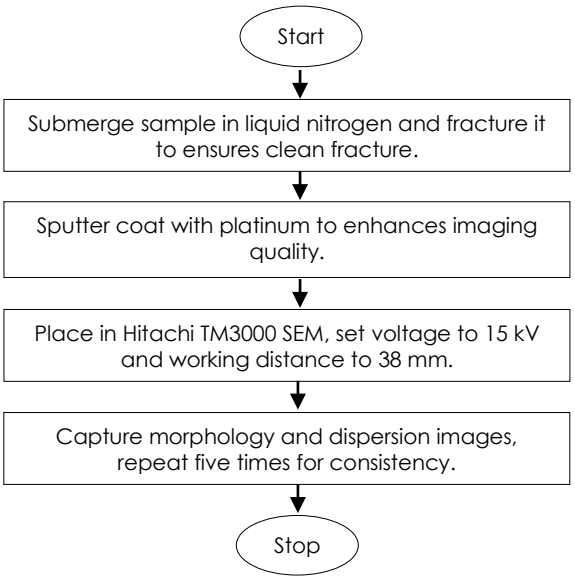

Figure 4 Flowchart of SEM Analysis Testing

SEM imaging was used to observe the dispersion of $ZnFe_2O_4$ particles and detect agglomeration, which can influence the electrical properties of the nanocomposites.

D. Electrical Breakdown

The dielectric breakdown voltage of both the AC and DC components was measured in accordance with ASTM D149 and ASTM D3755 standards, respectively. The breakdown testing was performed using a BAUR PGK 110B AC/DC High Voltage Test Set. For each nanocomposite formulation, three thin-film samples were prepared, with five measurement points on each sample, resulting in a total of fifteen breakdown measurements per formulation. Each sample had an average thickness of approximately 100 µm, with a tolerance of ±5%. To ensure independent and interference-free measurements, the points were spaced evenly across the sample surface, as demonstrated in Figure 5.

The flowchart in Figure 6 depicts the sequential steps involved in the experimental setup for measuring the dielectric breakdown voltage.

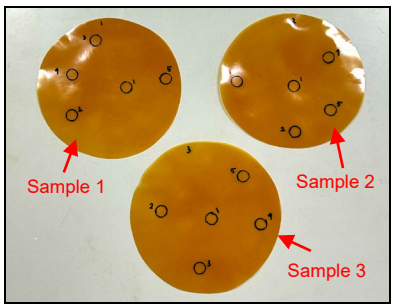

Figure 5 Example of Three PP/$ZnFe_2O_4$/2 Samples with Five Test Points Each for AC Breakdown Strength Testing

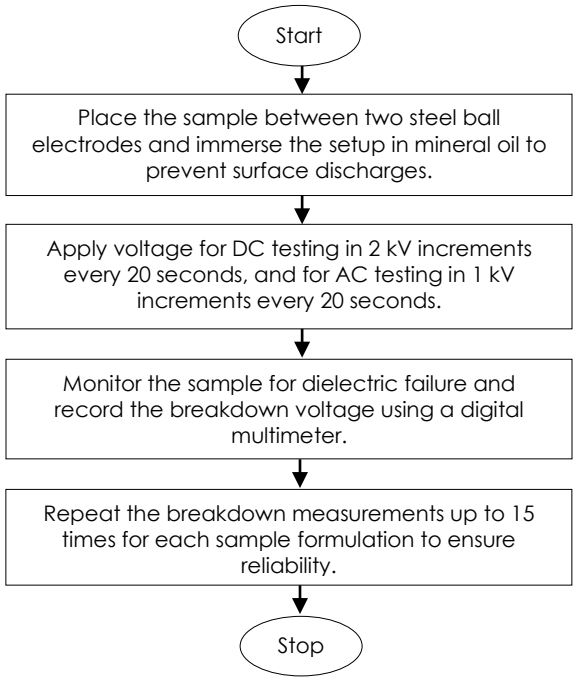

Figure 6 Flowchart of Dielectric Breakdown Analysis Testing

To assess the statistical reliability of the results, a two-parameter Weibull distribution method was applied to the breakdown data. For each sample, the breakdown voltage was recorded, and the average value was calculated. The breakdown strength was determined using Equation (1) [22], by dividing the measured breakdown voltage by the sample thickness. Statistical variation in the breakdown strength was further analyzed using the Weibull distribution, providing insights into the distribution and consistency of the breakdown strength values for each formulation.

$$\text{Breakdown Strength}\left(\frac{\text{kV}}{\text{mm}}\right) = \frac{\text{Breakdown Voltage (kV)}}{\text{Sample Thickness (mm)}} \quad (1)$$

Both AC and DC breakdown tests were chosen to evaluate the dielectric strength under different electric stress conditions, which is crucial for understanding the insulation performance in real-world applications.

3.0 RESULTS AND DISCUSSION

A. Differential Scanning Calorimetry

The thermal behavior of pure polypropylene (PP) and PP nanocomposites containing varying contents of zinc iron oxide ($ZnFe_2O_4$) nanofillers is summarized in Table 3. The differential scanning calorimetry (DSC) results indicate that the melting temperature (Tm) of all samples averages around 162°C, consistent with nanofillers not significantly impacting the crystalline structure of the PP, nor altering the thermal stability of the polymer matrix that encompasses it, which is in line with the research in [19]. The melting endotherms also exhibit identical narrow spikes, which further indicates that all the formulations have roughly the same level of crystallinity. Similarly, all the formulations exhibited nearly identical melting endotherms, confirming their comparable degree of crystallinity.

On the other hand, there are marked differences in the cooling behavior of the PP/$ZnFe_2O_4$. The crystallization temperature (Tc) in comparison to pure PP is approximately 118 °C. Similarly, the PP/$ZnFe_2O_4$ nanocomposite with 0.5 wt.% filler exhibits a comparable Tc of 118 °C, suggesting that the small filler content has minimal influence on the crystallization behavior. However, it increases with the increase of the content of $ZnFe_2O_4$. This is perceived to be due to the additive effect of the nanoparticles of $ZnFe_2O_4$, which decreases the amount of time consumed to form the crystal nucleates.

In particular, PP/$ZnFe_2O_4$ nanocomposites at larger filler loadings (2 wt.% and 5 wt.%) exhibit a higher crystallization temperature while pure PP has a comparatively lower crystallization temperature. The enhancement in the crystallization temperature indicates the function of the $ZnFe_2O_4$ as a nucleating agent, improving the rate of crystallization of the polymer matrix, with this effect increasing with greater amounts of filler because of the higher number of nucleation sites created by the suspended nanoparticles [23]. These findings are consistent with the study by Aizat et.al. [19], who also observed that the addition of inorganic nanoparticles did not significantly alter the melting temperature of PP but influenced its crystallization temperature due to the nucleation effect.

Table 3 Thermal Behavior of Pure PP and PP nanocomposites containing $ZnFe_2O_4$

Samples	Tm (°C)	Tc (°C)
PP/0	162	118
PP/$ZnFe_2O_4$/0.5	162	118
PP/$ZnFe_2O_4$/1	162	119
PP/$ZnFe_2O_4$/2	162	120
PP/$ZnFe_2O_4$/5	162	121

B. Scanning Electron Microscopy

In Figure 7(a), the SEM morphology of pure polypropylene (PP) corresponds with previously reported findings [19]. Nonetheless, the absence of significant phase segregation or particulate inclusions indicates that the matrix is homogeneous [24]. This uniformity is typical of pure PP, which contains few or no nanoparticles or fillers that could introduce heterogeneities. Additionally, the lack of significant phase separation suggests good compatibility between the two blend components, isotactic PP (PPh) and PP impact copolymer (PPi).

On the other hand, Figure 7 presents the SEM morphology of nanocomposites. At a lower filler concentration of 0.5 wt.%, a good dispersion of $ZnFe_2O_4$ down to approximately 100 nm is observable (as indicated by the arrows), demonstrating that the melt mixing process effectively disperses the $ZnFe_2O_4$ nanopowder throughout the nanocomposites. However, even at this low loading of 1 wt.%, noticeable nanoparticle agglomeration is evident, particularly in the circled regions. The use of spherical particles has resulted in some agglomeration due to stronger attractive forces between the particles, which created localized clusters that slightly distorted the polymer matrix.

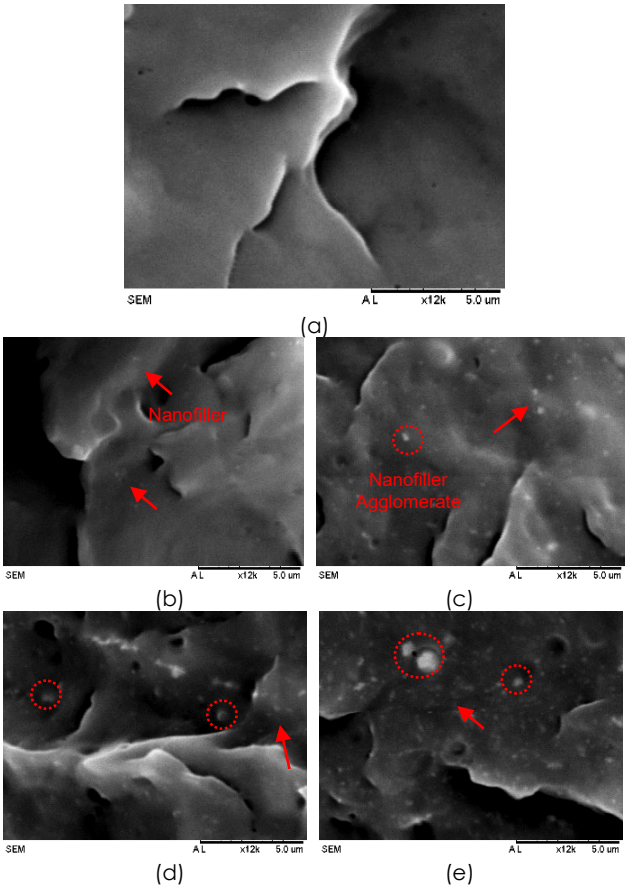

Figure 7 The SEM morphology of (a) Pure PP, (b) PP/$ZnFe_2O_4$/0.5, (c) PP/$ZnFe_2O_4$/1, (d) PP/$ZnFe_2O_4$/2, (e) PP/$ZnFe_2O_4$/5

As the concentration of $ZnFe_2O_4$ increases, agglomeration becomes more pronounced. At a concentration of 2 wt.%, the agglomerates are larger

and more frequent, with dimensions exceeding several micrometers. When the filler percentage reaches 5 wt.%, the SEM micrograph reveals a significant increase in nanoparticle clustering, resulting in the formation of large agglomerates. These agglomerates reduce the effective dispersion initially achieved with $ZnFe_2O_4$ in the resin and may lead to stress concentration, potentially impacting the dielectric and mechanical properties of the composite. The trend of increased agglomeration at higher filler contents agrees with previous reports [24], where metal oxide nanofillers such as TiO_2 or MgO also showed a tendency to form clusters beyond 3 wt.% loading.

C. Electrical Breakdown

The Weibull distribution analysis was conducted to evaluate the AC breakdown strength of various samples, with the results summarized in Table 4 and illustrated as a bar chart in Figure 8(a). The breakdown analysis provides two essential parameters, including the scale parameter (α), which shows the 63.2% failure probability strength level, and the shape parameter (β), which reveals breakdown strength consistency. Higher β values suggest a more uniform failure distribution, while lower values indicate greater variability in breakdown performance.

The AC breakdown strength results showed that pure PP exhibited the highest breakdown strength of 158 ± 8 kVmm^{-1} with a β value of 10 ± 4, indicating relatively high and consistent breakdown performance. The addition of $ZnFe_2O_4$ nanoparticles reduced the AC breakdown strength to 156 ± 10 kVmm^{-1} (0.5 wt.%), 150 ± 8 kVmm^{-1} (1 wt.%), 146 ± 11 kVmm^{-1} (2 wt.%), and 144 ± 10 kVmm^{-1} (5 wt.%). The decline in α suggests that the presence of nanofillers introduces structural inhomogeneities that weaken the dielectric strength, which is in line with the research in [26]. Despite the nucleating effect of $ZnFe_2O_4$, which improved crystallinity at lower filler loadings (0.5 wt.% and 1 wt.%), increasing the nanofiller content to 2 wt.% and 5 wt.% led to significant agglomeration, as observed in SEM images (previous result). These agglomerates disrupted the polymer matrix continuity, creating localized stress points that facilitated electrical failure [25]. The Weibull shape parameter (β) for AC breakdown followed a similar trend, decreasing from 10 ± 4 for pure PP to 7 ± 3 (0.5 wt.%), 9 ± 4 (1 wt.%), 6 ± 3 (2 wt.%), and 7 ± 3 (5 wt.%). The drop in β at higher filler concentrations suggests that agglomeration leads to greater variability in breakdown strength, likely due to non-uniform field distributions and localized defects.

The DC breakdown strength, shown in Figure 8(b) and Table 4, followed a similar trend, with pure PP showing the highest α value of 327 ± 10 kVmm^{-1} and a β value of 15 ± 6, indicating a high and consistent breakdown strength distribution. The incorporation of $ZnFe_2O_4$ nanoparticles led to a reduction in DC breakdown strength to 325 ± 27 kVmm^{-1} (0.5 wt.%), 289 ± 19 kVmm^{-1} (1 wt.%), 239 ± 22 kVmm^{-1} (2 wt.%), and 203 ± 23 kVmm^{-1} (5 wt.%). Compared to AC conditions, the reduction in DC breakdown strength was more pronounced, suggesting that DC breakdown is more sensitive to filler-induced structural inhomogeneities [26]. The β value for DC breakdown also exhibited a significant decline, dropping from 15 ± 6 for pure PP to 6 ± 2 (0.5 wt.%), 7 ± 2 (1 wt.%), 5 ± 2 (2 wt.%), and 2 ± 2 (5 wt.%). The lowest β value, recorded for the 5 wt.% sample indicates highly inconsistent breakdown strength, which can be attributed to charge accumulation around $ZnFe_2O_4$ agglomerates that act as conduction pathways under DC fields. Additionally, $ZnFe_2O_4$ nanoparticles may introduce polar surfaces that adsorb moisture, further enhancing electrical conduction and leading to space charge accumulation.

The Weibull analysis confirms that while $ZnFe_2O_4$ nanofillers influence dielectric breakdown properties, excessive filler content leads to increased structural variability and reduced reliability. At lower filler concentrations (0.5 wt.%), breakdown strength remains relatively stable, and β values suggest consistent performance. However, at higher filler loadings (2 wt.% and 5 wt.%), increased agglomeration significantly reduces both breakdown strength (α) and consistency (β), particularly under DC conditions. Similarly, a study by *Johari et al.* [26] also showed that adding too much MgO nanofiller to polypropylene reduced the DC breakdown strength. The highest strength was observed at 0.5 wt.% filler. When more filler was added, particle agglomeration occurred, which weakened the material.

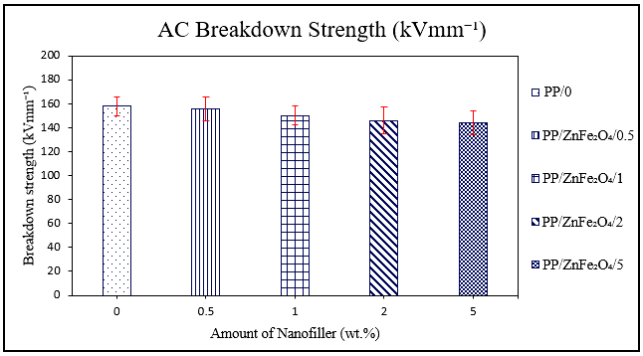

(a)

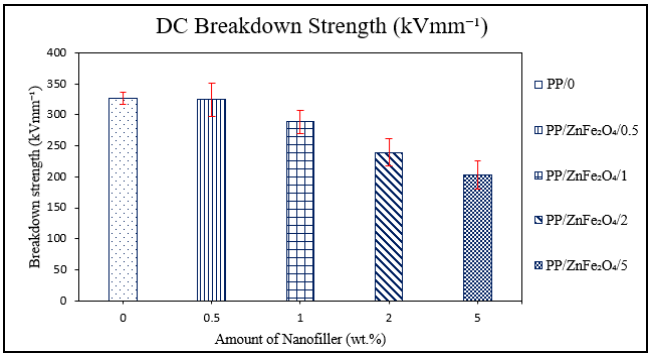

(b)

Figure 8 Bar Chart with Error Bars of (a) AC Breakdown Strength, and (b) DC Breakdown Strength

Table 4 AC and DC Breakdown Strength Parameters

Samples	AC		DC	
	α_{AC} (kVmm^{-1})	β_{AC}	α_{DC} (kVmm^{-1})	β_{DC}
PP/0	158 ± 8	10 ± 4	327 ± 10	15 ± 6
PP/$ZnFe_2O_4$/0.5	156 ± 10	7 ± 3	325 ± 27	6 ± 2
PP/$ZnFe_2O_4$/1	150 ± 8	9 ± 4	289 ± 19	7 ± 2
PP/$ZnFe_2O_4$/2	146 ± 11	6 ± 3	239 ± 22	5 ± 2
PP/$ZnFe_2O_4$/5	144 ± 10	7 ± 3	203 ± 23	2 ± 2

4.0 CONCLUSION

This work shows that the incorporation of $ZnFe_2O_4$ nanoparticles has a profound effect on the thermal and dielectric properties of PP nanocomposites. The nucleating effect caused by $ZnFe_2O_4$ enhances the crystallization tendency of the filler PP nanocomposites. Pure PP had the highest AC and DC breakdown strengths, while higher filler loadings (1 wt.%, 2 wt.%, and 5 wt.%) show a decrease in trends due to nanoparticle agglomeration as observed in the SEM result. Nevertheless, adding 0.5 wt.% of $ZnFe_2O_4$ results in comparable AC and DC breakdown strength to pure PP. These findings highlight the significance of optimizing the filler content and dispersion to achieve the desired thermal and dielectric performance in polymer nanocomposites.

However, certain limitations should be considered when interpreting these findings. The potential for uneven nanoparticle dispersion, especially at higher loadings, may influence the consistency of the results. In addition, the influence of processing parameters, such as mixing uniformity and sample preparation, might contribute to variability in thermal and electrical behavior. Moreover, this study focused on unaged samples; the long-term effects of environmental exposure or thermal aging were not covered. Future research should explore the role of processing techniques, filler surface modification, and durability under aging conditions to provide a more comprehensive understanding of the material's performance in real-world applications.

Acknowledgment

The authors would like to express their sincere gratitude to the Ministry of Education Malaysia, Universiti Teknologi Malaysia, UTMER, Q.J130000.3823.42J23, and the Nexus Young Researcher (NYR). The authors also thank the University Industry Research Laboratory (PPMU), UTM Johor Bahru, for the financial assistance provided for sample analysis.

Conflicts of Interest

The authors declare that there is no conflict of interest regarding the publication of this paper.

References

[1] Green, C. D., *et al.* 2015. Thermoplastic Cable Insulation Comprising a Blend of Isotactic Polypropylene and a Propylene-Ethylene Copolymer. *IEEE Transactions on Dielectrics and Electrical Insulation.* 22(2): 639–648. https://doi.org/10.1109/TDEI.2015.7076758.

[2] Diao, J., X. Huang, Q. Jia, F. Liu, and P. Jiang. 2017. Thermoplastic Isotactic Polypropylene/Ethylene-Octene Polyolefin Copolymer Nanocomposite for Recyclable HVDC Cable Insulation. *IEEE Transactions on Dielectrics and Electrical Insulation.* 24(3): 1416–1429. https://doi.org/10.1109/TDEI.2017.006208.

[3] Ketsamee, P., T. Andritsch, and A. Vaughan. 2023. The Effects of Humidity on Dielectric Permittivity of Surface-Modified TiO_2- and MgO-Based Polypropylene Nanocomposites. *IEEE Transactions on Dielectrics and Electrical Insulation.* 30(1): 82–89. https://doi.org/10.1109/TDEI.2022.3209640.

[4] Hu, S., *et al.* 2022. Comprehensive Comparisons of Grafting-Modified Different Polypropylene as HVDC Cable Insulation Material. *IEEE Transactions on Dielectrics and Electrical Insulation.* 29(5): 1865–1872. https://doi.org/10.3390/en16124701.

[5] Mahtabani, A., *et al.* 2021. Deposition of Ureido and Methacrylate Functionalities onto Silica Nanoparticles and Its Effect on the Properties of Polypropylene-Based Nanodielectrics. *IEEE Access.* 9: 130340–130352. https://doi.org/10.1109/ACCESS.2021.3112849.

[6] Xie, Y., Y. Zhao, G. Liu, J. Huang, and L. Li. 2019. Annealing Effects on XLPE Insulation of Retired High-Voltage Cable. *IEEE Access.* 7: 104344–104353. https://doi.org/10.1109/ACCESS.2019.2927882.

[7] Zhou, Y., J. He, J. Hu, X. Huang, and P. Jiang. 2015. Evaluation of Polypropylene/Polyolefin Elastomer Blends for Potential Recyclable HVDC Cable Insulation Applications. *IEEE Transactions on Dielectrics and Electrical Insulation.* 22(2): 673–681. https://doi.org/10.1109/TDEI.2015.7076762.

[8] Sharip, M. R. M., K. Y. Lau, M. A. M. Piah, D. N. A. Zaidel, S. A. Bhawani, and M. A. Talib. 2024. Structure and AC Breakdown Strength of Polypropylene/Ethylene-Octene Copolymer/Magnesium Oxide Nanocomposites. In *2024 IEEE 4th International Conference in Power Engineering Applications (ICPEA)*. 287–290. https://doi.org/10.1109/ICPEA60617.2024.10498222.

[9] Banerjee, A., N. Bose, and A. Lahiri. 2023. Effect of Zinc Oxide Nanofiller on the Dielectric Thermal and Optical Properties of Polypropylene. *IEEE Transactions on Industry Applications.* 59(1): 479–485. https://doi.org/10.1109/TIA.2022.3215955.

[10] Zhou, Y., *et al.* 2023. Enabling High-Performance Polypropylene Nanocomposites with Interfacial Deep Traps. *IEEE Transactions on Dielectrics and Electrical Insulation.* 30(1): 484–487. https://doi.org/10.1109/TDEI.2022.3229283.

[11] Ketsamee, P., T. Andritsch, and A. Vaughan. 2023. The Effects of Humidity on Dielectric Permittivity of Surface-Modified TiO_2- and MgO-Based Polypropylene Nanocomposites. *IEEE Transactions on Dielectrics and Electrical Insulation.* 30(1): 82–89. https://doi.org/10.1109/TDEI.2022.3209640.

[12] Rahim, N. H., K. Y. Lau, C. W. Tan, K. Y. Ching, and A. S. Vaughan. 2021. A Review of Engineering Dielectric Properties of Nanocomposites through Effectively Removed Interfacial Water. *IEEE Transactions on Dielectrics and Electrical Insulation.* 28(2): 448–459. https://doi.org/10.1109/TDEI.2020.009200.

[13] Cong, S., T. Lan, Y. Wang, L. Zu, S. Dong, and Z. Zhang. 2024. Preparation of High-Performance Anti-Aging Polypropylene by Modified Nano-TiO_2 and Calcium Sulfate Whisker Grafted Acrylonitrile Composite PP. *RSC*

Advances. 14(9): 6041–6047. https://doi.org/10.1039/d3ra08266k.

[14] Hones, H. M., J. T. Cook, M. J. McCaffrey, R. R. Krchnavek, and W. Xue. 2021. Effects of Material Preparation in Polyimide/SiO_2 Nanocomposites for Low-Temperature Dielectric Applications. *IEEE Transactions on Nanotechnology*. 20: 695–702. https://doi.org/10.1109/TNANO.2021.3112255.

[15] Ashokbabu, A., P. Thomas, D. Singh, and R. Vaish. 2022. Dielectric Properties of Polyaryletherketone/$CaCu_3Ti_4O_{12}$ Nanocomposite Films Fabricated via Cast Film Extrusion Process. *IEEE Transactions on Dielectrics and Electrical Insulation*. 29(4): 1324–1332. https://doi.org/10.1109/TDEI.2022.3188038.

[16] Zhu, X., Y. Zhou, Y. Zhang, L. Zhou, and X. Huang. 2022. The Effects of Nano-ZrO_2 on the Mechanical and Electrical Properties of Silicone Rubber and a Corresponding Mechanism Analysis. *IEEE Transactions on Dielectrics and Electrical Insulation*. 29(6): 2218–2226. https://doi.org/10.1109/TDEI.2022.3203373.

[17] Azmi, A., K. Y. Lau, C. W. Tan, R. Ayop, K. Y. Ching, and A. Vaughan. 2024. Aging-Resistant Breakdown Performance of Polypropylene Nanodielectrics. *IEEE Transactions on Dielectrics and Electrical Insulation*. 31(4): 1832–1839. https://doi.org/10.1109/TDEI.2024.3394830.

[18] Azmi, A., K. Y. Lau, N. A. Ahmad, Z. Abdul-Malek, C. W. Tan, K. Y. Ching, and A. Vaughan. 2022. Dielectric Properties of Thermally Aged Polypropylene Nanocomposites. *IEEE Transactions on Dielectrics and Electrical Insulation*. 29(2): 543–550. https://doi.org/10.1109/TDEI.2022.3163796.

[19] Azmi, A., K. Y. Lau, N. A. Ahmad, Z. Abdul-Malek, C. W. Tan, K. Y. Ching, and A. Vaughan. 2021. Structure Dielectric Property Relationship in Polypropylene/Multi-Element Oxide Nanocomposites. *IEEE Transactions on Nanotechnology*. 20: 377–385. https://doi.org/10.1109/TNANO.2021.3076663.

[20] Tabesh, F., S. Mallakpour, and C. M. Hussain. 2023. Recent Advances in Magnetic Semiconductor $ZnFe_2O_4$ Nanoceramics: History, Properties, Synthesis, Characterization, and Applications. *Journal of Solid State Chemistry*. 322: 123940. https://doi.org/10.1016/j.jssc.2023.123940.

[21] Raju, P., A. Thirupathi, C. Kalyani, S. M. Ali, J. Shankar, G. N. Rani, J. Anjaiah, and M. K. Durga. 2023. Synthesis and Thermal Stability of Ferrites Added Polymers Nanocomposites. *Materials Today: Proceedings*. 92: 1671–1675. https://doi.org/10.1016/j.matpr.2023.06.303.

[22] Azmi, A. 2019. Breakdown Characteristics of Polyethylene/Silicon Nitride Nanocomposites. *TELKOMNIKA Telecommunication Computing Electronics and Control*. 17(4): 1853–1858. https://doi.org/10.12928/telkomnika.v17i4.12754.

[23] Zhang, L., Y. Zhang, Y. Zhou, C. Teng, Z. Peng, and S. Spinella. 2018. Crystalline Modification and Its Effects on Dielectric Breakdown Strength and Space Charge Behavior in Isotactic Polypropylene. *Polymers*. 10(4): 406. https://doi.org/10.3390/polym10040406.

[24] Samad, A., K. Y. Lau, I. A. Khan, A. H. Khoja, M. M. Jaffar, and M. Tahir. 2018. Structure and Breakdown Property Relationship of Polyethylene Nanocomposites Containing Laboratory-Synthesized Alumina, Magnesia and Magnesium Aluminate Nanofillers. *Journal of Physics and Chemistry of Solids*. 120. https://doi.org/10.1016/j.jpcs.2018.04.036.

[25] Kolesov, S. N. 1980. The Influence of Morphology on the Electric Strength of Polymer Insulation. *IEEE Transactions on Electrical Insulation*. EI-15(5): 382–388. https://doi.org/10.1109/TEI.1980.298330.

[26] Johari, N. A., K. Y. Lau, Z. Abdul-Malek, M. R. M. Esa, C. W. Tan, and R. Ayop. 2023. Direct Current Breakdown Properties of Polypropylene Nanocomposites Containing Magnesium Oxide. In *2023 IEEE 3rd International Conference in Power Engineering Applications (ICPEA)*. 225–228. https://doi.org/10.1109/ICPEA56918.2023.10093176.